Tamoxifen Inhibits TRPV6 Activity via Estrogen Receptor–Independent Pathways in TRPV6-Expressing MCF-7 Breast Cancer Cells

Katrin A. Bolanz, Gergely Gy. Kovacs, Christopher P. Landowski, and Matthias A. Hediger

Institute of Biochemistry and Molecular Medicine, University of Bern, Switzerland

Abstract

The epithelial calcium channel TRPV6 is upregulated in breast carcinoma compared with normal mammary gland tissue. The selective estrogen receptor modulator tamoxifen is widely used in breast cancer therapy. Previously, we showed that tamoxifen inhibits calcium uptake in TRPV6-transfected *Xenopus* oocytes. In this study, we examined the effect of tamoxifen on TRPV6 function and intracellular calcium homeostasis in MCF-7 breast cancer cells transiently transfected with EYFP-C1-TRPV6. TRPV6 activity was measured with fluorescence microscopy using Fura-2. The basal calcium level was higher in transfected cells compared with nontransfected cells in calcium-containing solution but not in nominally calcium-free buffer. Basal influxes of calcium and barium were also increased. In transfected cells, 10 μmol/L tamoxifen reduced the basal intracellular calcium concentration to the basal calcium level of nontransfected cells. Tamoxifen decreased the transport rates of calcium and barium in transfected cells by 50%. This inhibitory effect was not blocked by the estrogen receptor antagonist, ICI 182,720. Similarly, a tamoxifen-induced inhibitory effect was also observed in MDA-MB-231 estrogen receptor–negative cells. The effect of tamoxifen was completely blocked by activation of protein kinase C. Inhibiting protein kinase C with calphostin C decreased TRPV6 activity but did not alter the effect of tamoxifen. These findings illustrate how tamoxifen might be effective in estrogen receptor–negative breast carcinomas and suggest that the therapeutic effect of tamoxifen and protein kinase C inhibitors used in breast cancer therapy might involve TRPV6-mediated calcium entry. This study highlights a possible role of TRPV6 as therapeutic target in breast cancer therapy.
(Mol Cancer Res 2009;7(12):2000–10)

Introduction

Breast cancer is still ranked third among all cancer deaths and had the highest incidence rate of all cancers of both sexes in Europe in 2006 (1). The survival chances of breast cancer patients depend to a great extent on the expression level and responsiveness of steroid hormone receptors in cancer tissues. Tumors that are estrogen receptor (ER) and progesterone receptor positive have a higher treatment success than those that are nonresponsive to estrogen and progesterone (2). The most widely used antiestrogen therapy is the application of tamoxifen, which belongs to the selective estrogen receptor modulators. Tamoxifen competitively inhibits estradiol binding to the ER and evokes a series of events such as conformational changes of the ER and dimerization and dissociation of heat shock proteins. This triggers binding of the ER to estrogen-responsive elements and transcriptional regulation. Additionally, many coregulator proteins can interact with the ER, but the exact mechanism of how tamoxifen effects the tumors and what role calcium plays in this process is not yet completely understood (3). There is also evidence that tamoxifen is cytotoxic for ER-negative breast cancer cells and that it can be effective in one third of ER-negative tumors (4, 5). A study by Bollig et al. (6) showed that tamoxifen upregulates protein phoshatase 1 α through an ER-independent pathway. Altered changes in intracellular Ca^{2+} were shown to be induced by tamoxifen at micromolar concentrations and to trigger death of breast cancer cells (7-10).

Changes in intracellular calcium homeostasis are a crucial step in tumor formation in every type of cancer because they influence several cellular functions such as cellular motility, differentiation, proliferation, and apoptosis. Furthermore, calcium is a key regulator of the cell cycle (11). Interestingly, there is an upregulation or downregulation of specific calcium channels or pumps associated with certain types of cancer. For instance, the plasma membrane ATPase 2 (PMCA2) is overexpressed in certain breast cancer cell lines such as ZR-75-1 compared with nontumorigenic 184B5 cells (12). In prostate cancer tumors, the expression level of TRPM8 mRNA is significantly increased in malignant tissue compared with healthy tissue (13). One other example is the altered expression of TRPV6 in prostate, pancreatic, thyroid, colon, ovary, and breast cancer (14).

TRPV6 belongs to the transient receptor potential (TRP) channels. The "TRPV" vanilloid subfamily comprises six channels of which TRPV5 and TRPV6 are relatively selective epithelial calcium channels expressed in renal tubular cells or in the apical membrane of enterocytes, respectively. TRPV6 was discovered in 1999 in rat duodenum using expression cloning

Received 5/6/09; revised 9/29/09; accepted 10/16/09; published OnlineFirst 12/8/09.
Grant support: Swiss National Science Foundation (M.A. Hediger), Bern Cancer League (C.P. Landowski), Novartis Foundation (M.A. Hediger), NIH/NCI (M.A. Hediger), and the Marie Curie Reintegration Grant (M.A. Hediger).
The costs of publication of this article were defrayed in part by the payment of page charges. This article must therefore be hereby marked *advertisement* in accordance with 18 U.S.C. Section 1734 solely to indicate this fact.
Note: K.A. Bolanz and G.G. Kovacs contributed equally to this work.
Requests for reprints: Matthias A. Hediger, Institute of Biochemistry and Molecular Medicine, University of Bern, Bern, Switzerland CH-3012. Phone: 41-31-631-4129; Fax: 41-31-631-3410. E-mail: matthias.hediger@mci.unibe.ch

doi:10.1158/1541-7786.MCR-09-0188

(15). Structurely, TRPV6 comprises 730 amino acids and contains six transmembrane domains and a short hydrophobic region between TM5 and TM6, which functions as the pore-forming region. The COOH terminus contains a calmodulin binding site and the NH_2 terminus has several ankyrin repeats on the intracellular side (16). TRPV6 is predominantly expressed in the duodenum where calcium is absorbed. *In situ* hybridization showed localization in the epithelial cells and on the villi tips (14). Additionally, TRPV6 expression was detected in pancreatic acinar cells, mammary gland duct cells, sweat glands, skin, and placenta (17). Examination of TRPV6 transport by electrophysiology revealed that the channel mediates passive Ca^{2+} transport with high calcium selectivity and an apparent K_m value for Ca^{2+} of 0.44 mmol/L. The cation permeability decreases in the order $Ca^{2+} > Ba^{2+} > Sr^{2+} > Mn^{2+}$ (18). At the present time, there is no selective blocker for TRPV6-mediated calcium influx available. Nonspecific blockage with ruthenium red, Gd^{3+}, and La^{3+} was observed (19). TRPV6 mRNA expression is regulated by dietary calcium, 1,25-vitamin D3, dihydrotestosterone, and estrogen (20-22). The intestinal calcium absorption is significantly reduced in TRPV6 knockout mice (23). This shows the importance of TRPV6 as a major calcium uptake pathway of dietary calcium in the intestine.

The exact function of TRPV6 in exocrine tissues is still unknown and its role in cancer is not clear thus far. Numerous studies are published on the role of TRPV6 in prostate cancer. A correlation of TRPV6 expression to the prostate cancer Gleason grade was detected in different cancer stages, whereas there was only little expression in normal prostate tissue (24). Furthermore, certain prostate cancer cell lines such as LNCaP and PC-3 express high amounts of TRPV6 mRNA (20). A study in LNCaP cells showed that TRPV6 can influence the proliferation rate, the cell cycle, and the expression of the proliferating cell nuclear antigen. TRPV6 is the main channel responsible for calcium uptake in this cell line and it can activate the nuclear factor of activated T-cells. Lehen'Kyi et al. (25) showed in the same study that the androgen receptor is involved in TRPV6 regulation in a ligand-independent way. They found that androgen receptor knockdown by siRNA decreased TRPV6 mRNA and protein levels, but the ligands DHT, an androgen receptor–selective agonist, and Casodex, a selective antagonist, had no significant effect on TRPV6 mRNA expression.

This confirms earlier results of studies using HEK293 cells, which revealed an increased proliferation rate if the cells were stably expressed with TRPV6 (26). Of great importance is the fact that TRPV6 mRNA and protein expression is not only increased in prostate cancer, but also in human carcinomas of the colon, thyroid, ovary, and breast (14, 20, 27).

In the ductal epithelial cells of the mammary gland, TRPV6 was found to be expressed in the apical membrane (14).

Our former study confirmed that TRPV6 is expressed at higher levels in breast cancer samples compared with nontumorous samples (28). We also showed that TRPV6 expression in T47D breast cancer cells is increased by estrogen, progesterone, and 1,25-vitamin D3. In contrast, tamoxifen was found to downregulate TRPV6 expression in cancer cells and to inhibit radioactive calcium uptake into TRPV6-expressing *Xenopus* oocytes. Therefore, TRPV6 might be involved in the mechanism of tamoxifen in breast cancer cells. In T47D cells, TRPV6 is able to control proliferation as we showed using the siRNA expression knockdown targeting TRPV6. The studies indicated that it might be clinically useful to develop specific TRPV6 inhibitors as breast cancer drugs. Especially, in the case of ER-negative tumors, TRPV6 targeting could be promising (28).

As a continuation of our published article on the role of TRPV6 in breast cancer, in the present study, our goal was to show the inhibitory effect of tamoxifen on TRPV6-mediated calcium uptake in breast cancer cells and to investigate the mechanism and the subsequent effect on intracellular calcium homeostasis. Our findings help to clarify a potential mechanism of how tamoxifen may be useful in breast cancer therapy.

Results

Expression of TRPV6 in MCF-7, T47D ER+, and MDA-MB-231 ER– Breast Cancer Cells

First, we tested the expression of TRPV6 mRNA in three widely used human breast cancer cell lines. TRPV6 mRNA was found to be expressed at a high level in T47D cells, whereas MCF-7 and MDA-MB-231 cells showed very low levels of TRPV6 (Fig. 1A). The amount of TRPV6 mRNA expressed in T47D was comparable with the mRNA level in LNCaP prostate cancer cells (data not shown). Immunoprecipitation of TRPV6 followed by Western blot technique revealed that T47D cells express higher levels of TRPV6 protein compared with the other two cell lines (Fig. 1B). When we examined the level of the expressed TRPV6 protein qualitatively in these three cell lines using immunofluorescence microscopy, our observation was similar as shown in Fig. 1C. Furthermore, in T47D cells, TRPV6 showed colocalization with PMCA, suggesting that it is expressed at the plasma membrane (Fig. 2).

Effect of Tamoxifen on Calcium Entry in T47D Cells

The basal calcium influx was determined by measuring the rate of the increase of the fura-2 fluorescence ratio following administration of 1 mmol/L calcium. In T47D cells, this calcium influx was very small (Fig. 3A and C). When we investigated the effect of 10 μmol/L tamoxifen on basal calcium influx, we found a remarkable increase in calcium entry (Fig. 3B and C). Additionally, tamoxifen induced a large transient increase in intracellular calcium in nominally calcium-free buffer (Fig. 3B).

These effects can be explained by the fact that tamoxifen induces calcium depletion of the endoplasmic reticulum calcium stores, which in turn activates store-operated calcium channels (SOCC) expressed in the plasma membrane. This phenomenon was observed in several other cell types. Unfortunately, the activation of SOCCs masks any possible effect of tamoxifen on TRPV6. Therefore, we had to turn to another approach namely overexpressing EYFP-tagged TRPV6 in MCF-7 cells.

Effect of Tamoxifen on TRPV6-Mediated Calcium Entry in MCF-7 Cells

MCF-7 cells were chosen for transfection of TRPV6 because they express only very low levels of endogenous TRPV6 (Fig. 1A). Confocal, fluorescence images of transfected MFC-7

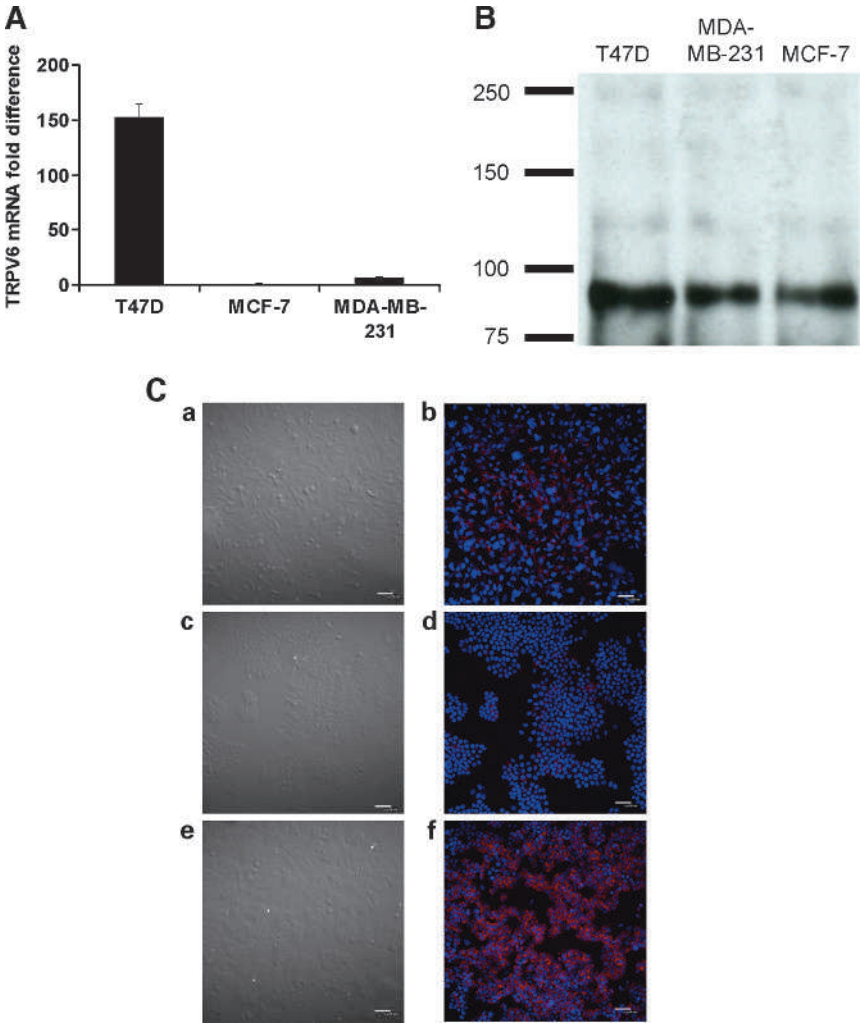

FIGURE 1. **A.** Comparison of TRPV6 mRNA expression (fold difference) in MCF-7, MDA-MB-231 cells, and T47D human breast cancer cells detected with real-time PCR. **B.** Comparison of TRPV6 protein in T47D, MDA-MB-231, and MCF-7 cells measured with immunopreciptiation and Western blotting. **C.** Phase contrast images (*left*) and immunofluorescence staining (*right*) of TRPV6 in MDA-MB-231 cells (*a* and *b*), MCF-7 (*c* and *d*), and T47D cells (*e* and *f*). Images were taken with a ×20 objective (*scale bar,* 20 μm).

cells suggested that exogenous TRPV6 is expressed at the plasma membrane (Fig. 4, *arrows*). The transfected cells were identified based on EYFP fluorescence (Fig. 5A and B).

As expected, the basal intracellular calcium concentration was highly increased in transfected cells, compared with nontransfected cells (ratio of 2.027 ± 0.023 versus 1.23 ± 0.004; $P < 0.001$; Figs. 5C, 6A and B). When extracellular calcium was omitted, this difference was no longer detectable (1.16 ± 0.004 versus 1.116 ± 0.002). Furthermore, basal calcium and barium influx was 100- and 9- fold larger in transfected cells compared with nontransfected cells, respectively (Fig. 6C and D).

Basal intracellular calcium concentrations and the basal calcium influx rate correlated closely, as shown in Fig. 6E and F. Both of the influxes were almost completely inhibited by 100 μmol/L Gd^{3+}, a nonspecific TRPV6 inhibitor (data not shown). Our functional data and confocal images provided solid evidence that the expressed EYFP-TRPV6 is fully functional at the plasma membrane.

Incubation with 10 μmol/L tamoxifen for 10 minutes induced a transient calcium increase followed by a sustained decrease in intracellular calcium. The intracellular calcium in transfected cells finally reached the calcium level of nontransfected cells (Fig. 7A). In nominally calcium-free medium, the tamoxifen-induced calcium increase was reduced to insignificant levels (Fig. 7B).

The application of 10 μmol/L tamoxifen for 10 minutes induced a prominent decrease in initial calcium and barium influx rate down to 37.6% (ratio of 440.84 ± 45.84 versus 165.77 ± 26.39, respectively) and 39.7%, respectively (ratio of 90.75 ± 9.00 versus 36.04 ± 3.20; Fig. 6C and D). Tamoxifen at 1 μmol/L for 1 hour also decreased TRPV6 activity to 24.4% (ratio of 440.84 ± 45.84 versus 107.63 ± 16.04) but not when applied for 10 minutes (Fig. 8). Furthermore, the tamoxifen metabolite, 4-hydroxy-tamoxifen (10 μmol/L for 10 minutes), decreased TRPV6 activity to 17.77% (ratio of 440.84 ± 45.84 versus 78.32 ± 13.74; Fig. 8).

Determination Whether the Estrogen Receptor Is Involved in the Observed Effect of Tamoxifen

When the ER antagonist ICI 182,780 (1 μmol/L) was applied together with tamoxifen to MCF-7 cells, we observed no significant change of the tamoxifen-induced inhibition in

the presence of ICI 182,780 (Fig. 9A). To confirm these findings, we examined the effect of 10 μmol/L tamoxifen in the ER-negative, human breast cancer cell line, MDA-MB-231, transiently transfected with EYFP-C1-TRPV6. Tamoxifen exerted a similar effect such as in transfected MCF-7 cells. The initial calcium influx was decreased to 30.5% by tamoxifen in transfected cells compared with the control group (ratio of 542.28 ± 157.58 versus 165.73 ± 32.29; Fig. 9B).

Determination Whether Protein Kinase C Plays a Role in the Observed Effect of Tamoxifen

Because tamoxifen was shown to affect protein kinase C (PKC) activity in MCF-7 cells and several possible serin/threonine phosphorylation sites can be predicted on TRPV6, we tested whether PKC inhibition could be involved in the effect of tamoxifen on TRPV6 activity (29). We found that activation of PKC with 200 nmol/L phorbol 12-myristate 13-acetate (PMA) promptly elevated intracellular calcium in transfected cells, whereas the effect was much smaller in nontransfected cells. Furthermore, in some transfected cells, slow calcium oscillations could be observed (Fig. 10A). When extracellular calcium was removed, this robust calcium increase vanished. Also, basal calcium influx was significantly increased in the transfected cells (Fig. 10A). The inhibitory effect of tamoxifen was completely abolished in the presence of PMA (Fig. 10B). When we applied the PKC inhibitor calphostin C (100 nmol/L), we observed that calphostin C alone or in combination with tamoxifen decreased the initial calcium influx in transfected MCF-7 cells to 40.5% and 46.4%, respectively (from 440.84 ± 45.84 to 178.57 ± 21.99, to 204.34 ± 30.56; Fig. 10B). Therefore, tamoxifen exerted no additional inhibitory effect when PKC was inhibited.

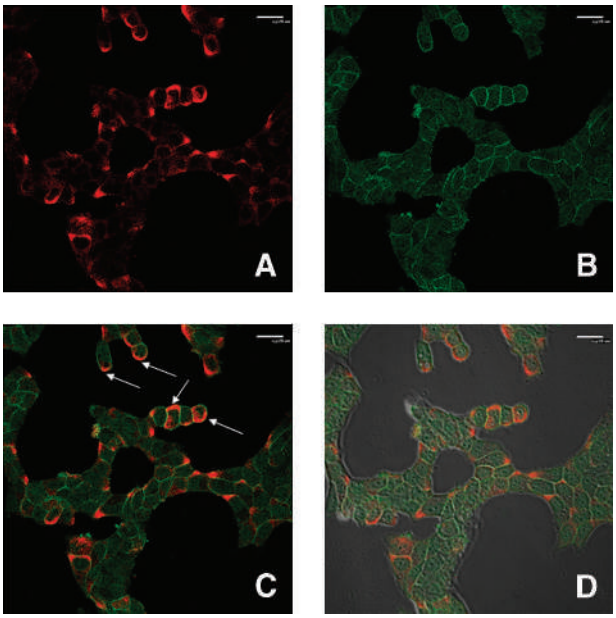

FIGURE 2. Immunofluorescence double staining with anti-TRPV6 (**A**) and anti-PMCA antibodies (**B**) in T47D cells. Arrows, the colocalization of TRPV6 and PMCA in the merged (**C**) image. **D.** The overlay of the phase contrast and the merged image. Images were taken with a ×20 objective (*scale bar,* 20 μm).

Discussion

In spite of intensive efforts toward development of novel therapeutic approaches for the prevention and treatment of breast cancer, the incidence rate of breast adenocarcinomas is still highest among all cancer types and the mortality rate was third among all cancers in Europe in 2006 (1). Because intracellular calcium plays a critical role in many fundamental cellular processes such as proliferation, apoptosis, and secretion, calcium levels are spatially and temporally tightly controlled in cells. Disturbances in intracellular calcium homeostasis are a crucial factor in the process of tumor progression in all cancer types. Many studies have been conducted to evaluate how the regulatory system of intracellular calcium homeostasis and the associated calcium signaling pathways are altered in breast cancer cells compared with normal mammary gland cells. A recent review summarizes the possible roles of T-type calcium channels in breast cancer progression (30). The essential roles of the SOCC Orai1 and the signaling molecule Stim1 in breast cancer metastasis formation was recently reported (31). Monteith and his group (12) observed that the expression of different isoforms of the PMCA is changed in breast cancer cells and that PMCA2 expression is significantly increased (32). Furthermore, inhibition of PMCA using siRNA decreased proliferation of MCF-7 human breast cancer cells (33). In recent years, there has been accumulating evidence that the TRPV6 epithelial calcium entry channel is involved in breast cancer progression. In human and mouse breast cancer samples, TRPV6 protein expression was increased (14).

In addition, our laboratory recently showed that a knockdown of TRPV6 expression using siRNA decreased basal calcium influx and proliferation of T47D human breast cancer cells (28). As a novel finding, we also found that tamoxifen, at micromolar levels, inhibits TRPV6-mediated calcium influx in human TRPV6-expressing *Xenopus* oocytes. In the present study, we addressed the mechanism of this inhibitory effect and its consequences on intracellular calcium homeostasis using transfected breast cancer cell lines.

We selected two widely used human, ER-positive breast cancer cell lines, T47D and MCF-7, and MDA-MB-231, which are ER-negative. First, we examined the expression of TRPV6 in these cell lines. The mRNA levels were low in MCF-7 and MDA-MB-231 and high in T47D cells. The expression of TRPV6 in T47D cells was comparable with LNCaP prostate cancer cells, which are known to have high TRPV6 levels (data not shown). Immunofluorescence staining and Western blotting of immunoprecipitated samples also showed much higher expression of TRPV6 in T47D cells compared with MCF-7 or MDA-MB-231 cells. Unfortunately, in T47D cells, a high dose of tamoxifen above 1 μmol/L induced depletion of the ER calcium stores followed by a robust increase in SOCC activity. Because, in nondepolarizing cells, the majority of the basal calcium influx occurs through SOCC, the possible effect of tamoxifen on native TRPV6 activity was masked. Tamoxifen also exerts the same effect on SOCC activity in several cell types such as human oral cancer cells, CHO-K1 cells, human osteosarcoma cells, and ZR-75-1 human breast cancer cells (34-37). This effect was shown not to be mediated by ERs.

To evaluate the effect of tamoxifen on TRPV6, we increased the number of TRPV6 channels residing in the plasma

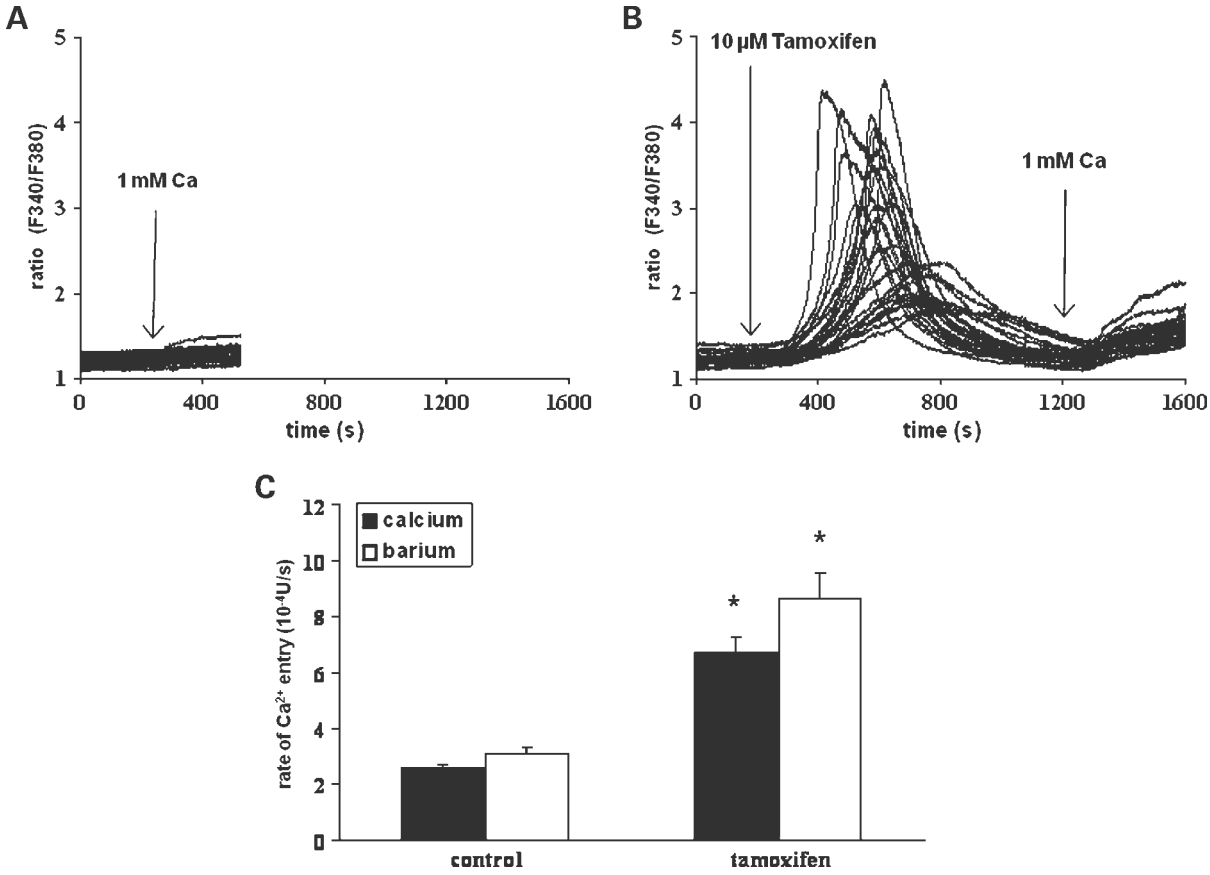

FIGURE 3. Representative tracings (**A** and **B**) and bar graph (**C**) showing the effect of 10 μmol/L tamoxifen citrate on basal barium and calcium influxes in T47D cells. Number of separate experiments, >6; *, $P < 0.05$.

membrane of the MCF-7 cells, which expresses a low level of endogenous TRPV6. To this end, we overexpressed EYFP-tagged human TRPV6 in MCF-7 cells to reach expression levels of TRPV6 comparable with those of SOCCs. In such TRPV6-overexpressing cells, we observed a significantly higher basal calcium level and increased calcium and barium influxes. Confocal immunofluorescence studies confirmed that TRPV6 is expressed at the plasma membrane. A short, 10-minute incubation of 10 μmol/L tamoxifen induced a much higher transient calcium response in transfected cells compared with nontransfected cells, the effect of which was diminished when extracellular calcium was omitted.

It should be noted that we selected this initial tamoxifen concentration because the IC_{50} value of tamoxifen was 7.5 μmol/L in *Xenopus* oocytes (28).

In transfected MCF-7 cells, after transient calcium elevation, basal intracellular calcium returned to the same level as in nontransfected cells. As described above, this temporary calcium elevation is probably due to ER calcium store depletion and subsequent activation of SOCCs. In transfected cells,

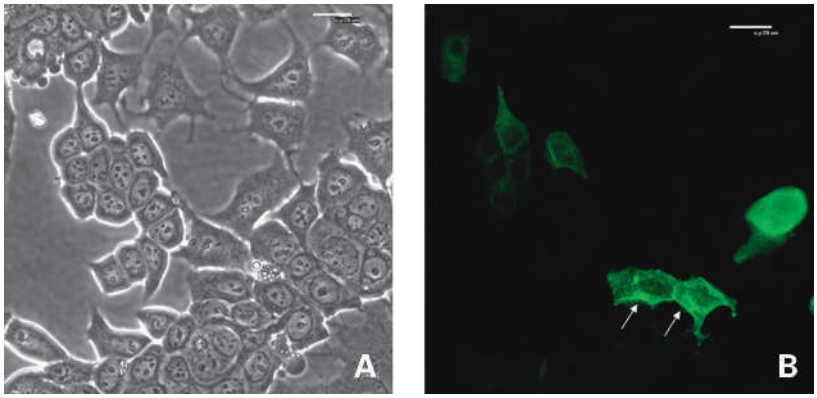

FIGURE 4. Phase contrast (**A**) and fluorescence EYFP image (**B**) to display localization of EYFP-C1-TRPV6 after transient transfection in MCF-7 cells. Images were taken with a ×60 objective (*scale bar,* 20 μm). Arrows, plasma membrane localization.

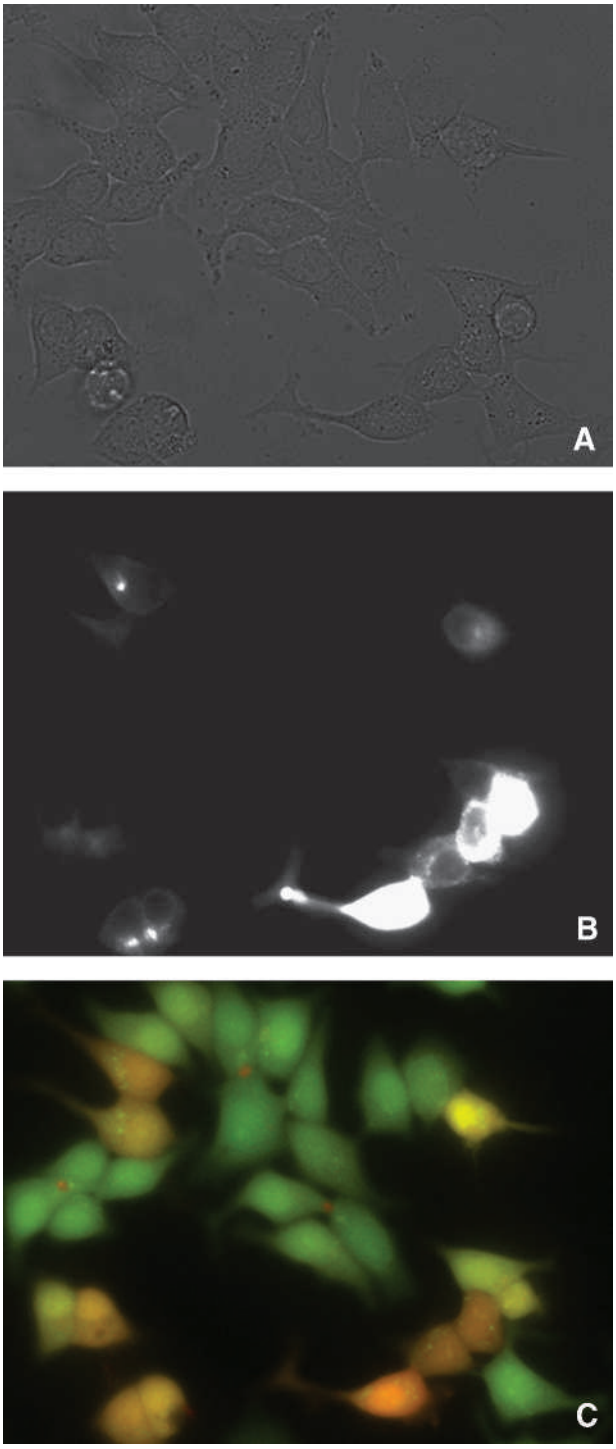

FIGURE 5. Phase contrast image (**A**), EYFP image (**B**), and Fura-2 ratio image (**C**) of EYFP-C1-TRPV6–expressing MCF-7 cells. Note that TRPV6-expressing cells have higher basal intracellular calcium level.

both basal calcium and barium influxes were reduced by tamoxifen to 37.6% and 39.7%, respectively. In nontransfected cells, there was either no effect (barium influx) or a small increase (calcium influx) in response to tamoxifen. Hydroxytamoxifen (10 μmol/L) and prolonged incubation with lower (1 μmol/L) dose of tamoxifen also reduced TRPV6-mediated calcium influx, suggesting that in tamoxifen-treated breast cancer patients, inhibition of TRPV6 could be involved in the antitumor effect of tamoxifen. After treatment of patients with 5 or 20 mg tamoxifen citrate daily for 28 days, the concentration of tamoxifen can reach between 0.73 and 2 μmol/L in the breast cancer tissue (38). In our experiments, we used 10 μmol/L tamoxifen and, to further ensure the physiologic significance, also a lower concentration of tamoxifen (1 μmol/L).

As we expected, ERs were not involved because inhibition of ERs with ICI 182,780 in ER+ MCF-7 cells was ineffective. Also, tamoxifen reduced TRPV6 activity in the ER-negative cell line, MDA-MB-231, to the same extent as in the ER-positive cell line, MCF-7.

Previously, it was shown that tamoxifen is a potent PKC inhibitor *in vitro* (39). However, in MCF-7 cells, the reported findings on the effect of tamoxifen are controversial. Rowlands et al. tested the inhibitory potential of several tamoxifen analogues in MCF-7 cells (29). In 2003, one group observed a reduction of PKC activity by tamoxifen, whereas in another report, an increased PKC activity and induction of PKC translocation to the plasma membrane in response to tamoxifen was observed (40, 41). The phosphorylation of T702 on TRPV6 by PKC was also shown by Flockerzi and his group (42). This threonine residue is localized in the calmodulin binding site of TRPV6. Phosphorylation at this position blocks inactivation of the channel by calcium-calmodulin complex. In our experiments, activation of PKC by PMA completely abolished the inhibitory effect of tamoxifen on TRPV6. When the PKC inhibitor calphostin C (100 nmol/L) was applied, TRPV6 activity was diminished. Furthermore, tamoxifen had no inhibitory effect in the presence of calphostin C. It was shown previously that calphostin C can reduce MCF-7 cell viability very potently (43). However, because TRPV6-mediated barium entry was also inhibited by tamoxifen, and because barium does not bind to calmodulin (44), we conclude that tamoxifen does not inhibit TRPV6 function through augmentation of calmodulin-mediated inactivation. Nevertheless, there are several other possible sites on TRPV6 predicted to be phosphorylated by PKC. Phosphorylation of one or more of these could enhance TRPV6-mediated ion influx.

In summary, we show that tamoxifen inhibits TRPV6 activity via an ER-independent way. This finding may help to explain the mechanism behind the success in therapy of ER-negative breast tumors with tamoxifen. Although the detailed mechanism of how tamoxifen affects TRPV6 still needs to be elucidated, we conclude that PKC activity modulates the inhibitory effect of tamoxifen. We also found that PKC activation enhances, whereas PKC inhibition decreases, TRPV6 activity, and that these effects are not mediated by calmodulin. It is tempting to suggest that PKC inhibitors used for breast cancer treatment affect TRPV6 as well. Our findings suggest that TRPV6 might be a possible target for the development of new breast cancer medications.

Materials and Methods

Materials

The breast cancer cell lines, MCF-7, MDA-MB-231 and T47D were obtained from American Type Culture Collection,

Health Protection Agency, and NIH National Cell, respectively. Culture Center. Fugene 6 transfection reagent was used from Roche Applied Biosystems. The EYFP-C1-hTRPV6 vector was a generous gift from Prof. Christoph Romanin, Institute for Biophysics, Johannes Kepler Universität Linz, Austria.

Rabbit anti-human TRPV6 antibody was obtained from ProteinTech Group, Inc. Mouse anti-human PMCA antibody was purchased from Abcam. Hoechst 33342, goat anti-rabbit IgG conjugated to Alexa 594, goat anti-mouse IgG conjugated to Alexa 488, Fura-2 AM, cell culture medium RPMI 1640, and cell culture reagents were obtained from Invitrogen. The mounting medium Citifluor AF2 was from LucernaChem. Tamoxifen citrate was purchased from Acros Organics, and ICI 182,780 was from Tocris Bioscience. Phorbol-12-myristate-13-acetate and calphostin C were purchased from Calbiochem. All other chemicals were obtained from Sigma-Aldrich). Anti-rabbit IgG horseradish peroxidase conjugate (Promega), Amersham enhanced chemiluminescence Western Blotting Detection Reagents (GE Healthcare), Complete Mini (protease inhibitors; Roche Diagnostics GmbH), Immobilon-P Transfer Membrane (Milian), and 1% Nonidet P-40 (Roche Diagnostics GmbH) were used for the Western blotting and immunopreciptation.

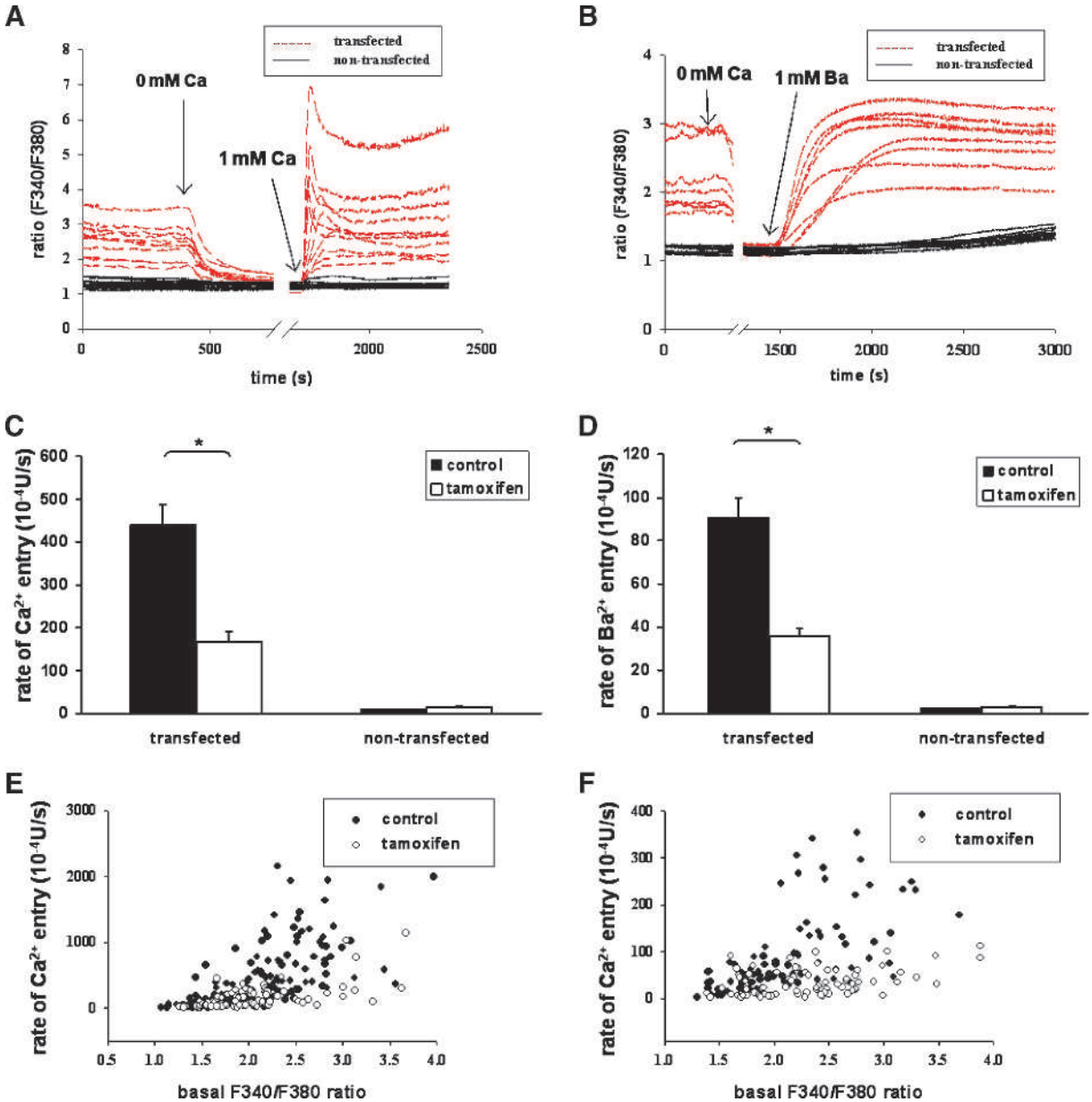

FIGURE 6. Representative tracings showing Ca^{2+} (**A**) and Ba^{2+} (**B**) influxes in MCF-7 cells using the Ca^{2+}-sensitive fluorescent dye fura-2. First, extracellular Ca^{2+} was removed followed by administration of 1 mmol/L external Ca^{2+} or Ba^{2+} when the fura-2 ratio was stabilized. The rate of the increase of the fura-2 ratio in response to readdition of the particular divalent cation was analyzed. Summary data in **C** and **D** show the rate of changes in Fura-2 ratio after readdition of calcium or barium with or without 10 μmol/L tamoxifen citrate treatment for 10 min in transfected and nontransfected cells. **E** and **F.** The correlation between basal calcium or barium entry and normal intracellular calcium concentration in transfected cells. *, $P < 0.05$ control versus tamoxifen group.

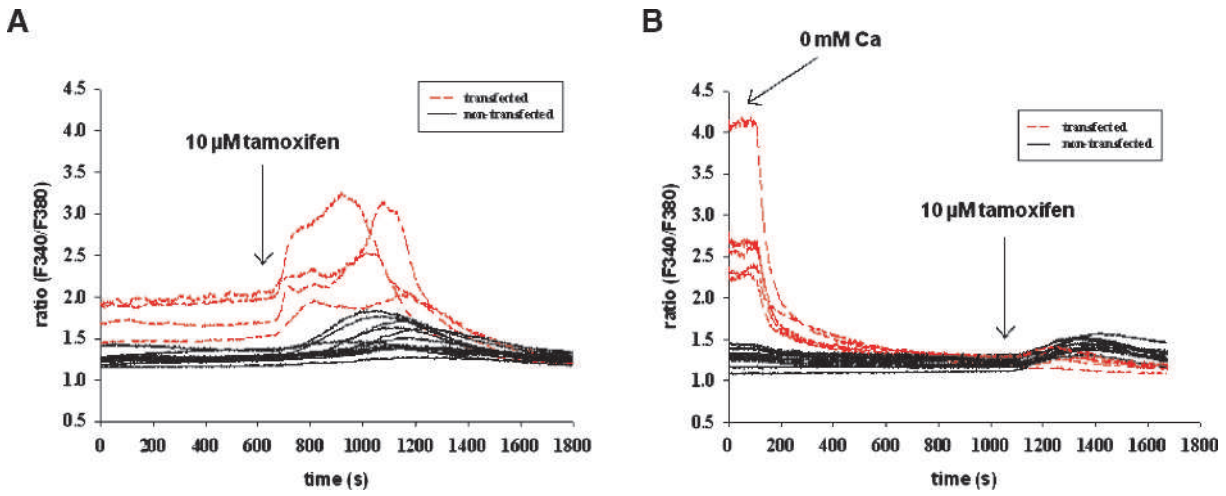

FIGURE 7. Representative tracings showing the effect of 10 μmol/L tamoxifen citrate on intracellular $[Ca^{2+}]$ ($[Ca^{2+}]_i$) in EYFP-C1-TRPV6–expressing MCF-7 cells in the presence of 1 mmol/L extracellular Ca^{2+} (**A**) or in nominally calcium-free solution (**B**).

Cell Culture

The human breast cancer cells lines MCF-7 and T47D were cultured in RPMI medium supplemented with 10% fetal bovine serum, 1 mmol/L HEPES, and 1% penicillin/streptomycin. The cells were kept in a cell culture incubator at 5% CO_2 at 37°C and were passaged twice a week.

Real-time PCR

cDNA was prepared for every sample by reverse transcription of total RNA isolated with Trizol using TaqMan Reverse Transcription Reagents (Applied Biosystems) according to the manufacturer's manual. For all experiments, mRNA expression was measured by real-time PCR using an Applied Biosystems 7500 Real-time PCR System. Reactions consisted of 1× Mastermix, 0.9 μmol/L forward and reverse primers, and 0.2 μmol/L dual-labeled fluorescent probes each for TRPV6 and β-actin. The sequences of the forward and reverse primers for TRPV6 were 5′-GGT TCC TGC GGG TGG AA-3′ and 5′-CCT GTG CGT AGC GTT GGA T-3′, respectively, with the resulting amplicon being 62 bp with a temperature of 60°C. The sequence of the probe for TRPV6 was 5′-ACA GGC AAG ATC TCA ACC GGC AGC-3′. The sequences of the forward and reverse primers for β-actin were 5′-CCT GGC ACC CAG CAC AAT-3′ and 5′-GCC GAT CCA CAC GGA ATA CT-3′, respectively, with the resulting amplicon being 69 bp with a temperature of 60°C. The sequence of the probe for β-actin was 5′-ATC AAG ATC ATT GCT CCT CCT GAG CGC-3′. The specificity of all primers was confirmed by BLAST search. Primer Express (Applied Biosystems) was used for designing primers for TRPV6 and β-actin. All primers were designed to cross exon-exon boundaries of the coding sequence. Primers were optimized and validated for the comparative Ct method, as described in the manufacturer's manual. ABI Prism SDS software version 1 was used for the analysis of the amplification plots. The fold change ± SD in TRPV6 expression was normalized to β-actin.

Immunoprecipitation and Western Blotting

Three confluent 100-mm cell culture dishes of T47D, MDA-MB-231, and MCF-7 cells were washed thrice with ice-cold PBS. Cells were lysed in lysis buffer (composition: 10 mmol/L

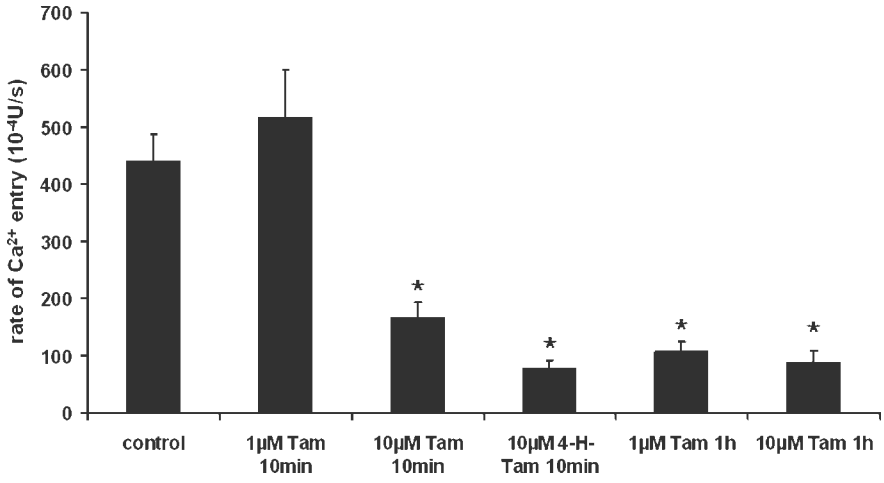

FIGURE 8. Summary data showing the rate of changes in the fura-2 ratio after readdition of calcium in control group and in response to treatment with 1 μmol/L tamoxifen (*Tam*), 10 μmol/L tamoxifen, and 10 μmol/L 4-hydroxy-tamoxifen (*4-H-Tam*) treatment for 10 min and with 1 and 10 μmol/L tamoxifen treatment for 1 h in MCF-7 cells transfected with TRPV6. *, $P < 0.05$ treatment versus control group.

Tris-HCl, 150 mmol/L NaCl, 10 mmol/L MgCl, 1% Nonidet P-40, and protease inhibitor cocktail) for 30 min at 4°C under constant agitation. Samples were centrifuged at 12,000 rpm for 20 min at 4°C, and the protein concentration of the saved supernatant was adjusted to 2 mg/mL. Thereafter, 1 mL of the supernatant was incubated with 4 μg of rabbit anti-TRPV6 antibody for 1 h under rotary agitation at 4°C. The samples were then mixed with 30 μL of agarose protein G beads, and the mixture was incubated overnight at 4°C. Beads were washed thrice with lysis buffer, and afterwards, 40 μL of 2× loading buffer were added. The samples were boiled at 95°C for 5 min and run on a 6% SDS-PAGE. The samples were transferred with a semidry method to a polyvinylidene difluoride membrane, and blocked with 5% milk, 0.5% bovine serum albumin, and 0.02% sodium azide in PBS overnight at 4°C. The blocked membrane was probed with the same anti-TRPV6 antibody at 1:500 dilution for 2 h at room temperature and washed thrice in PBS with 0.1% Tween 20. An horseradish peroxidase–conjugated goat anti-rabbit secondary antibody (1:20,000) was applied for 1 h at room temperature. After three washes in PBS with 0.1% Tween 20 and one final wash in PBS, enhanced chemiluminescence was used to visualize the bands on the membrane.

Immunofluorescence

Three days before staining, MCF-7 and T47D cells (150.000 cells per well) were seeded on poly-D-lysine–coated coverslips in six-well plates. All the following steps were done at RT. First, the cells were rinsed twice with TBS and then fixed with 4% PFA in TBS for 15 min. Subsequently, they were washed thrice for 10 min with TBS and blocked with TBS supplemented with 10% goat serum for 1 h. Then, incubation with rabbit anti-TRPV6 (1:100) in TBS with 0.5% bovine serum albumin and 0.02% NaN_3 for 90 min followed by three washes with TBS for 10 min was done. The cells were stained with mouse anti-PMCA (1:500) for 1 h in the same buffer followed by the same washing procedure. The cells were incubated first with a goat anti-rabbit secondary antibody conjugated to Alexa 594 and then with a goat anti-mouse secondary antibody conjugated to Alexa 488 at 1:4,000 dilution in TBS with 0.5% bovine

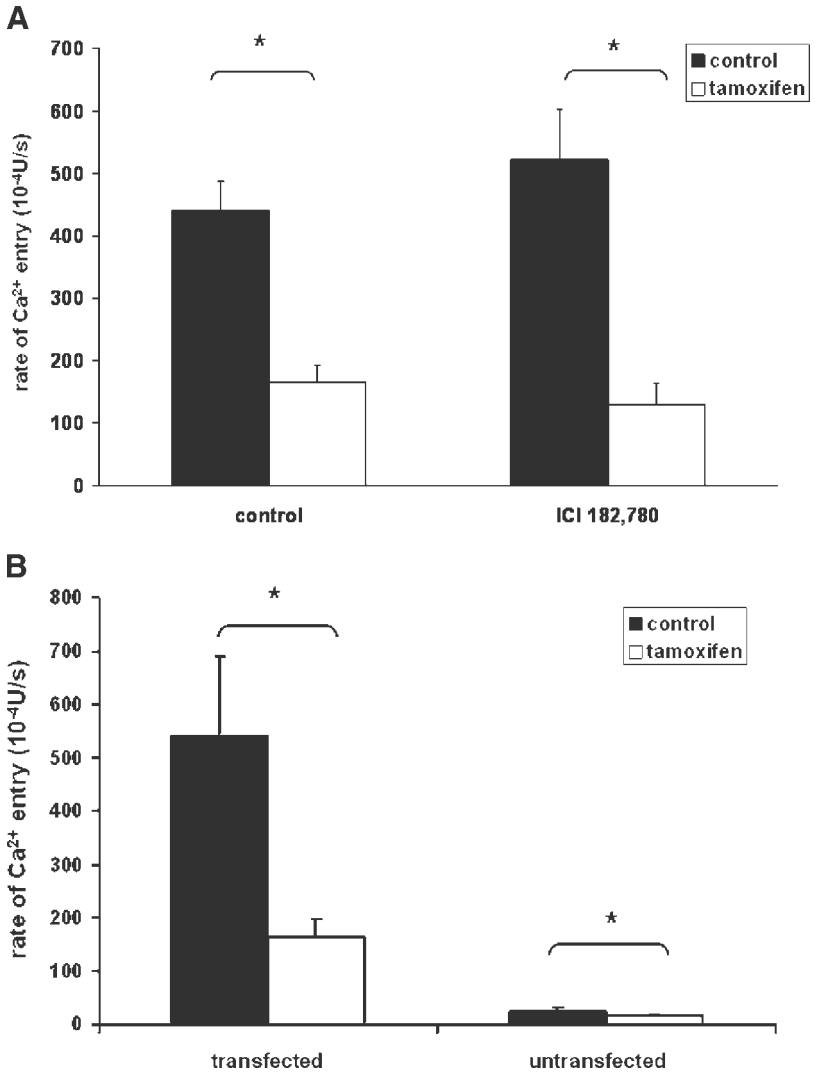

FIGURE 9. A. Effect of pretreatment of transfected MCF-7 cells with the ER antagonist ICI 182.780 (1 μmol/L) for 10 min on TRPV6 activity with and without tamoxifen. Data are the means of at least 25 cells from six separate experiments. **B.** Effect of 10 μmol/L tamoxifen on calcium influx in ER-negative MDA-MB-231 cells. *, $P < 0.05$ control versus tamoxifen group.

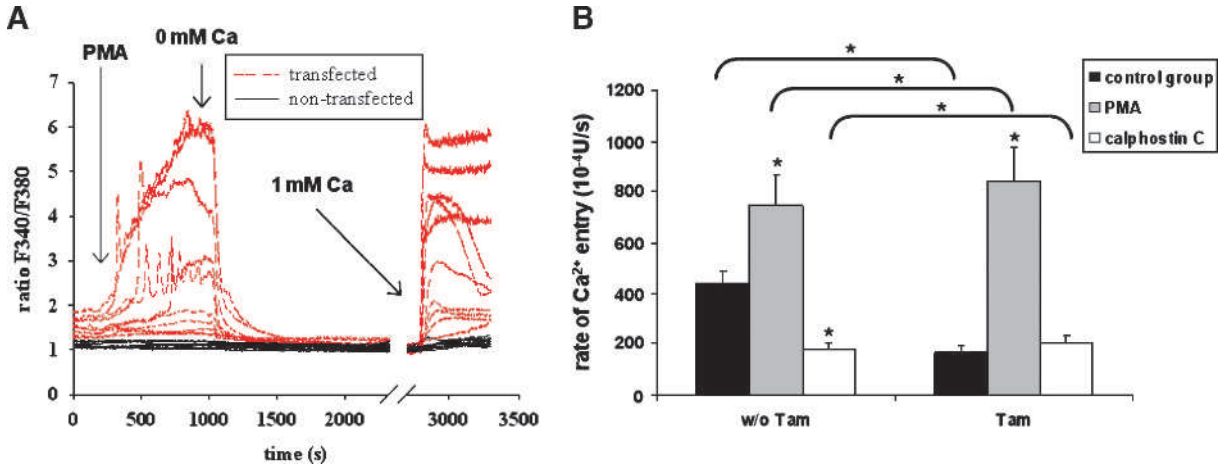

FIGURE 10. **A.** Representative tracings showing changes in the calcium increase induced by inhibition of PKC with 200 nmol/L PMA for 10 min. **B.** Summary data showing the effect of the PKC activator PMA (200 nmol/L) and the PKC inhibitor calphostin C (100 nmol/L) on the inhibitory effect of 10 μmol/L tamoxifen in MCF-7 cells transfected with TRPV6. Cells were pretreated with calphostin C for 1 h. Data are the means of at least 25 cells from six separate experiments. *, $P < 0.05$ treatment versus control group.

serum albumin and 0.02% NaN_3 for 1 h separated by three 10-min washes with TBS. Then, the cells were washed thrice for 10 min and mounted with CityFluor AF2. For staining of EYFP-TRPV6–transfected cells, Fugene 6 was applied 48 h after seeding according to the manufacturer's manual. After transfection, cells were incubated for 24 to 48 h before fixing and mounting the cells as described above.

Confocal Imaging

The slides were imaged with a confocal, laser scanning microscope setup using a Nikon Eclipse TE2000-E fully automatized inverted, epifluorescence microscope outfitted with Nikon D-Eclipse C1 laser confocal optics. The system equipped with a violet-diode (405 nm) and a multiline Argon (457-515 nm) from Melles Griot, and a Helium/Neon (594 nm) lasers from JDS Uniphase. Nikon EZ-C1 3.6 confocal imaging software installed on a HP xw4400 workstation was used for image acquisition. Brightness and contrast were adjusted with ImageJ.

Ion Imaging

For calcium imaging, breast cancer cells (300,000 cells per well) were seeded on poly-D-lysine–treated coverslips in 35-mm dishes. After 24 h, they were transfected with EYFP-TRPV6 plasmid using Fugene 6 according to the manufacturer's manual. After transfection, cells were incubated for 24 to 48 h before ionic imaging.

Cell were loaded with 2.5 μg/mL Fura-2 acetoxy-methyl ester dissolved in DMSO containing PluroniC F-1278 20% in serum-free RPMI in cell culture incubator for 1 h. Cells were incubated in calcium containing Krebs buffer for 20 min. For calcium and barium measurement, Fura-2 ratios (F340/F380) were monitored. All measurements were background corrected. The calcium imaging was done on a Nikon Eclipse Ti-U microscope equipped with a Polychrome V+ monochromator (TILL Photonics). A Nikon ×40 SFluor objective was used for visualization. Images were captured with a Hamamatsu Orca-ER monochrome CCD camera. Image acquisition and analysis was done using Simplepci version 6.2 from CImaging. Basal calcium or barium entry was measured as the rate of the increase of Fura-2 ratio in response to the administration of 1 mmol/L divalent cation into nominally calcium-free solution.

Statistics

Data are presented as mean ± SEM. Nontransfected groups were compared with Mann-Whitney rank sum test. Spearmans rank correlation test and Fisher's z transformation were used in case of testing significance between transfected groups. Differences in the comparison tests lower than $P < 0.05$ or $Z_{0.05} > 1.96$ were considered significant.

Disclosure of Potential Conflicts of Interest

No potential conflicts of interest are disclosed.

Acknowledgments

We thank statistician Pasquale Cirillo PhD, Institute of Mathematical Statistics and Actuarial Sciences, University of Bern, for helpful discussion about data analysis.

References

1. Ferlay J, Autier P, Boniol M, et al. Estimates of the cancer incidence and mortality in Europe in 2006. Ann Oncol 2007;18:581–92.

2. Lippman MA, Fauci AS, Braunwald E, Kasper DL, Hauser SL, Loscalzo J. Breast Cancer 2008.17th Edition (Chapter 86). http://www.accessmedicine.com/content.aspx?aID=2877884.

3. Ellis MJ, Swain SM, Chabner BA, Longo DL. Steroid hormone therapies for cancer. 3rd ed. 2001, p. 103–13.

4. Dowsett M, Houghton J, Iden C, et al. Benefit from adjuvant tamoxifen therapy in primary breast cancer patients according oestrogen receptor, progesterone receptor, EGF receptor and HER2 status. Ann Oncol 2006;17:818–26.

5. Mandlekar S, Yu R, Tan TH, Kong AN. Activation of caspase-3 and c-Jun NH2-terminal kinase-1 signaling pathways in tamoxifen-induced apoptosis of human breast cancer cells. Cancer Res 2000;60:5995–6000.

6. Bollig A, Xu L, Thakur A, et al. Regulation of intracellular calcium release and PP1α in a mechanism for 4-hydroxytamoxifen-induced cytotoxicity. Mol Cell Biochem 2007;305:45–54.

7. Decensi A, Robertson C, Viale G, et al. A randomized trial of low-dose tamoxifen on breast cancer proliferation and blood estrogenic biomarkers. J Natl Cancer Inst 2003;95:779–90.

8. Furr BJ, Jordan VC. The pharmacology and clinical uses of tamoxifen. Pharmacol Ther 1984;25:127–205.

9. MacCallum J, Cummings J, Dixon JM, Miller WR. Concentrations of tamoxifen and its major metabolites in hormone responsive and resistant breast tumours. Br J Cancer 2000;82:1629–35.

10. Peyrade F, Frenay M, Etienne MC, et al. Age-related difference in tamoxifen disposition. Clin Pharmacol Ther 1996;59:401–10.

11. Monteith GR, McAndrew D, Faddy HM, Roberts-Thomson SJ. Calcium and cancer: targeting Ca2+ transport. Nat Rev Cancer 2007;7:519–30.

12. Lee WJ, Roberts-Thomson SJ, Monteith GR. Plasma membrane calcium-ATPase 2 and 4 in human breast cancer cell lines. Biochem Biophys Res Commun 2005;337:779–83.

13. Fuessel S, Sickert D, Meye A, et al. Multiple tumor marker analyses (PSA, hK2, PSCA, trp-p8) in primary prostate cancers using quantitative RT-PCR. Int J Oncol 2003;23:221–8.

14. Zhuang L, Peng JB, Tou L, et al. Calcium-selective ion channel, CaT1, is apically localized in gastrointestinal tract epithelia and is aberrantly expressed in human malignancies. Lab Invest 2002;82:1755–64.

15. Peng JB, Chen XZ, Berger UV, et al. Molecular cloning and characterization of a channel-like transporter mediating intestinal calcium absorption. J Biol Chem 1999;274:22739–46.

16. Nijenhuis T, Hoenderop JG, Bindels RJ. TRPV5 and TRPV6 in Ca(2+) (re) absorption: regulating Ca(2+) entry at the gate. Pflugers Arch 2005;451:181–92.

17. Suzuki Y, Landowski CP, Hediger MA. Mechanisms and regulation of epithelial Ca2+ absorption in health and disease. Annu Rev Physiol 2008;70:257–71.

18. Yue L, Peng JB, Hediger MA, Clapham DE. CaT1 manifests the pore properties of the calcium-release-activated calcium channel. Nature 2001;410:705–9.

19. Goyer RA. Toxic and essential metal interactions. Annu Rev Nutr 1997;17:37–50.

20. Peng JB, Zhuang L, Berger UV, et al. CaT1 expression correlates with tumor grade in prostate cancer. Biochem Biophys Res Commun 2001;282:729–34.

21. Song Y, Peng X, Porta A, et al. Calcium transporter 1 and epithelial calcium channel messenger ribonucleic acid are differentially regulated by 1,25 dihydroxyvitamin D3 in the intestine and kidney of mice. Endocrinology 2003;144:3885–94.

22. Van Cromphaut SJ, Rummens K, Stockmans I, et al. Intestinal calcium transporter genes are upregulated by estrogens and the reproductive cycle through vitamin D receptor-independent mechanisms. J Bone Miner Res 2003;18:1725–36.

23. Bianco SD, Peng JB, Takanaga H, et al. Marked disturbance of calcium homeostasis in mice with targeted disruption of the Trpv6 calcium channel gene. J Bone Miner Res 2007;22:274–85.

24. Fixemer T, Wissenbach U, Flockerzi V, Bonkhoff H. Expression of the Ca2+-selective cation channel TRPV6 in human prostate cancer: a novel prognostic marker for tumor progression. Oncogene 2003;22:7858–61.

25. Lehen'Kyi V, Flourakis M, Skryma R, Prevarskaya N. TRPV6 channel controls prostate cancer cell proliferation via Ca2+//NFAT-dependent pathways. Oncogene 2007;26:7380–5.

26. Schwarz EC, Wissenbach U, Niemeyer BA, et al. TRPV6 potentiates calcium-dependent cell proliferation. Cell Calcium 2006;39:163–73.

27. Wissenbach U, Niemeyer BA, Fixemer T, et al. Expression of CaT-like, a novel calcium-selective channel, correlates with the malignancy of prostate cancer. J Biol Chem 2001;276:19461–8.

28. Bolanz KA, Hediger MA, Landowski CP. The role of TRPV6 in breast carcinogenesis. Mol Cancer Ther 2008;7:271–9.

29. Rowlands MG, Budworth J, Jarman M, et al. Comparison between inhibition of protein kinase C and antagonism of calmodulin by tamoxifen analogues. Biochem Pharmacol 1995;50:723–6.

30. Taylor JT, Zeng XB, Pottle JE, et al. Calcium signaling and T-type calcium channels in cancer cell cycling. World J Gastroenterol 2008;14:4984–91.

31. Yang S, Zhang JJ, Hunag XY. Orai1 and STIM1 are critical for breast tumor cell migration and metastasis. Cancer Cell 2009;15:124–34.

32. Lee WJ, Roberts-Thomson SJ, Holman NA, et al. Expression of plasma membrane calcium pump isoform mRNAs in breast cancer cell lines. Cell Signal 2002;14:1015–22.

33. Lee WJ, Robinson JA, Holman NA, et al. Antisense-mediated Inhibition of the plasma membrane calcium-ATPase suppresses proliferation of MCF-7 cells. J Biol Chem 2005;280:27076–84.

34. Lu YC, Jiann BP, Chang HT, et al. Effect of the anti-breast cancer drug tamoxifen on Ca2+ Movement in human osteosarcoma cells. Pharmacol Toxicol 2002;91:34–9.

35. Chu ST, Huang CC, Huang CJ, et al. Tamoxifen-induced $[Ca^{2+}]_i$ rises and Ca^{2+}-independent cell death in human oral cancer cells. J Recept Signal Transduct Res 2007;27:353–67.

36. Chang HT, Huang JK, Wang JL, et al. Tamoxifen-induced increases in cytoplasmic free Ca2+ levels in human breast cancer cells. Breast Cancer Res Treat 2002;71:125–31.

37. Jan CR, An-Jen C, Chang HT, et al. The anti-breast cancer drug tamoxifen alters Ca2+ movement in Chinese hamster ovary (CHO-K1) cells. Arch Toxicol 2003;77:160–6.

38. Kisanga ER, Gjerde J, Guerrieri-Gonzaga A, et al. Tamoxifen and metabolite concentrations in serum and breast cancer tissue during three dose regimens in a randomized preoperative trial. Clin Cancer Res 2004;10:2336–43.

39. O'Brian CA, Liskamp RM, Solomon DH, Weinstein IB. Inhibition of Protein Kinase C by Tamoxifen. Cancer Res 1985;45:2462–5.

40. Cabot MC, Zhang Z, Cao H, et al. Tamoxifen activates cellular phospholipase C and D and elicits protein kinase C translocation. Int J Cancer 1997;70:567–74.

41. Boyan BD, Sylvia VL, Frambach T, et al. Estrogen-dependent rapid activation of protein kinase C in estrogen receptor-positive MCF-7 breast cancer cells and estrogen receptor-negative HCC38 cells is membrane-mediated and inhibited by tamoxifen. Endocrinology 2003;144:1812–24.

42. Niemeyer BA, Bergs C, Wissenbach U, Flockerzi V, Trost C. Competitive regulation of CaT-like-mediated Ca2+ entry by protein kinase C and calmodulin. Proc Natl Acad Sci U S A 2001;98:3600–5.

43. Guo B, Hembruff SL, Villeneuve DJ, Kirwan AF, Parissenti AM. Potent killing of paclitaxel- and doxorubicin-resistant breast cancer cells by calphostin C accompanied by cytoplasmic vacuolization. Breast Cancer Res Treat 2003;82:125–41.

44. Thyagarajan B, Lukacs V, Rohacs T. Hydrolysis of phosphatidylinositol 4,5-bisphosphate mediates calcium–induced inactivation of TRPV6 channels. J Biol Chem 2008;283:14980–7.